Dehydrogenation of Ethylbenzene in Presence of Carbon Dioxide Over Supported Fe₂O₃-Cr₂O₃ Mixed Oxides Catalysts

Ahmed Aouissi[*], Hoceine Bayahia, Zeid A. Al-Othman and M. Rafiq H. Siddiqui

Department of Chemistry, College of Science, King Saud University, Riyadh, Kingdom of Saudi Arabia

*Corresponding author: E-mail: aouissed@yahoo.fr

Dehydrogenation of ethylbenzene to styrene in the presence of carbon dioxide was investigated over a series of binary iron-chromium oxides (Fe₂O₃-Cr₂O₃) supported on alumina, silica and titania. The catalysts were characterized by means of XRD, IR and SEM. XRD and FT-IR characterization indicated that iron and chromium ions are dispersed into the support matrix. Compared to Fe-Cr-Si-30 and Fe-Cr-Ti-30 catalysts, Fe-Cr-Al-30 was found to be the most active (conversion = 57.2 %) and the most selective in styrene (94.1 %). The activity value was observed in the following order Fe-Cr-Al > Fe-Cr-Ti.> Fe-Cr-Si. SEM images indicated that there are no significant carbonaceous deposits on the spent Fe-Cr-Al-30 catalyst, whereas modifications of its morphological aspect were observed. The variation of Fe-Cr content in the Fe-Cr-Al catalysts showed that the activity depends strongly on the content. The optimal content determined was 50 wt- %.

Keywords: Mixed oxides, Ethylbenzene dehydrogenation, Styrene, Carbon dioxide, Support.

INTRODUCTION

Styrene is one of the most important monomer for synthetic polymers. More than 90 % of its world production is obtained by the dehydrogenation of ethylbenzene (EB). Currently, the dehydrogenation of EB is carried out at 600-700 ºC, just below the temperature where thermal cracking becomes significant on the promoted iron oxide catalysts[1,2]. Due to the highly endothermic and volume increasing character of the reaction, a large amount of superheated steam is required to supply heat, lower the partial pressure of the reactant, thus shifting the chemical equilibrium to higher styrene formation[3-5]. The large amount of wasted energy in the form of excess steam[6], the thermodynamic equilibrium limitations and the deactivation of catalyst[5] are among the several problems which must be solved[7]. In order to circumvent some of these cited difficulties, the process of dehydrogenation of EB using CO₂ instead of steam has received much attention[8-12]. This process, if developed is believed to be an energy-saving and environmentally friendly process. In fact, the oxidative dehydrogenation of EB with CO₂ as a soft oxidant[13] possesses several advantages[10,14-17] than O₂ (strong oxidant) which leads the production of undesired by-products (oxygenates) along with styrene[18]. It is well known that in the present commercial iron catalyst, hematite (α-Fe₂O₃) is preferred for styrene production. Small amounts of other metal oxides like Cr₂O₃ are added as promoters[19]. However,

this commercial iron based catalyst does not work effectively for the ethylbenzene in the presence of CO₂. Consequently various supports such as Al₂O₃, MgO, WO₃, SiO₂, ZrO₂ and activated carbon have been tested on the dehydrogenation of EB in the presence of CO₂[20-30]. It has been found that Fe or Cr oxides supported on activated carbon and Fe oxide supported on ZrO₂ exhibited high initial catalytic activity, but suffered from severe deactivation[22,23,28,31]. Saito *et al.*[32] found that EB was activated by the acidic sites over γ-Al₂O₃ supported catalysts while CO₂ was activated by basic sites; CO₂ conversion was then correlated with the amounts of strong basic sites. The acid-basic and redox properties of the catalyst, at an optimum composition, will influence the conversion and selectivity to styrene[24,29]. Strong basic sites lead to the toluene formation, whereas acidic ones lead to the benzene formation[33]. In this work, the performance of the binary oxides Fe-Cr catalyst system for the dehydrogenation of EB with CO₂ has been investigated. The effect of the support and Fe-Cr loading on the support was explored.

EXPERIMENTAL

Catalysts preparation: The supported catalysts were prepared by the wet impregnation method. Typically, the support (alumina, silica and titania) was impregnated with aqueous mixture solution of 1 M Cr(NO₃)₃·9H₂O and 1 M Fe(NO₃)₃·6H₂O. The volumes of the mixture solution were

selected to obtain Fe/Cr = 10/90 (molar ratio) in the final binary oxides. Three catalysts, α-Fe_2O_3-Cr_2O_3-Al_2O_3, α-Fe_2O_3-Cr_2O_3-SiO_2 and α-Fe_2O_3-Cr_2O_3-TiO_2, referred to as Fe-Cr-Al-30, Fe-Cr-Si-30 and Fe-Cr-Ti-30 constituted of 30 % by weight of the binary oxides Fe-Cr in the catalyst were prepared by stirring the support and impregnation solutions maintained at 50 °C until dryness evaporation and then dried overnight at 120 °C. The precursor salt was calcined at 750 °C in stainless steel reactor with air flow of 6 L/h. The sample was heated first to 120 °C for 0.5 h then the temperature was increased to 750 °C for 3.5 h.

Catalysts characterization: Powder X-ray diffraction patterns were obtained on a Siemens D5000 diffractometer with CuK_{α} (λ = 1.5418 Å) radiation. Fourier transform-infrared spectra of the samples were recorded with Shimadzu FTIR Spetrometer 8400S at ambient conditions *via* grinding the sample with KBr and then pressed. Scanning electron microscopy and elemental analysis (Energy Dispersive X-Ray Analysis: EDAX) were carried out using Jeol SEM model JSM 6360A (Japan).

Catalyst testing: The dehydrogenation of EB in the presence of CO_2 was carried out in flow fixed bed reactor loaded with a sample of catalyst under atmospheric pressure. Prior to dehydrogenation of EB, a sample of a mixed oxides catalyst was pretreated at 700 °C for 1 h with 50 mL min^{-1} CO_2 gas. Then, the reactant mixture CO_2 and EB at a flow rate of 50 mL min^{-1} was passed through the catalyst at 660 °C. The molar ratio of CO_2 to EB was fixed at 11.7 and the W/F was controlled at 13.9 gcat h/mol. The flow of CO_2 gas was controlled by mass flow controller. Ethylbenzene was fed to the reaction system with syringe pump. The reaction products were analyzed with a gas phase chromatograph (Agilent 6890N) equipped with a flame ionization detector, a thermal conductivity detector and a capillary column (HP-PLOT Q length 30 m ID 0.53 mm).

RESULTS AND DISCUSSION

X-Ray powder diffraction: The XRD patterns of samples with different compositions calcined at 750 °C are shown in Fig. 1. Phase identification was performed by comparing the experimental XRD pattern results (Fig. 1) with the reported XRD data in ICDD (International Centre for Diffraction Data) and JCPDS (Joint Committee on Powder Diffraction Standards). The mixed oxides, Cr-Fe-10, showed the typical XRD pattern of Cr_2O_3 and α-Fe_2O_3 with hematite structure (JCPDS files No. 33-664 and 38-1479, respectively). The peaks are relatively sharp and strong indicating crystalline product with relatively large crystallites. Nevertheless, other phases could be present as traces. In fact, it has been reported for several oxides, the
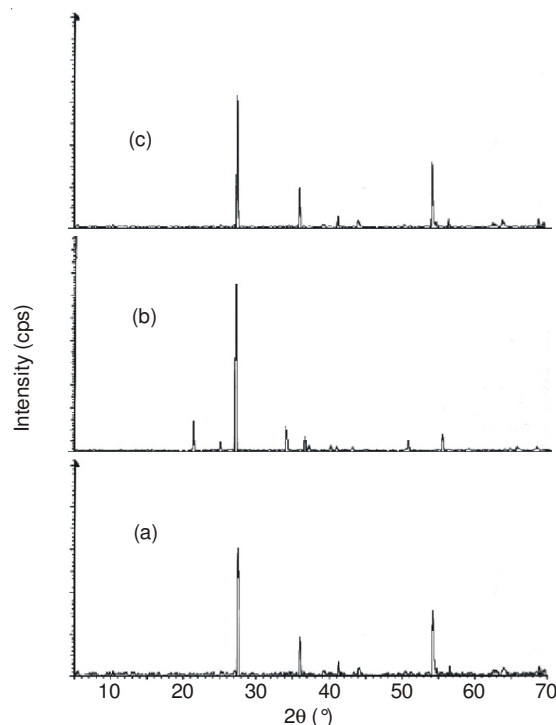

Fig. 1.   XRD patterns of the supported Fe-Cr binary oxides calcined at 750 °C: (a) Fe-Cr-Al-30; (b) Fe-Cr-Si-30; (c) Fe-Cr-Ti-30

coexistence of various phases besides the main phase[26,27]. The XRD results indicated that the mixed oxides have slightly different values than the unsupported binary oxides depending on the support. Table-1 presents the d-spacings that correspond to the most significant peaks in the patterns of the unsupported and the supported binary oxides. The deviation from the corresponding unsupported binary oxides, α-Fe_2O_3 and Cr_2O_3, respectively may suggest that some iron and chromium ions are dispersed into the support matrix.

FTIR analysis: The mixed oxides were characterized by FT-IR spectroscopy. The IR spectra of the samples in the range from 4000-400 cm^{-1} are shown in Fig. 2. The IR band at 3464 cm^{-1} corresponds to the stretching vibrations of adsorbed H_2O molecules. The IR band at 1626 band is normally attributed to O-H bending vibrations[34]. Compared with the unsupported α-Fe_2O_3/Cr_2O_3 mixed oxides, the supported ones showed almost the same features in their FT-IR spectra that can be attributed to changes in the metal-oxygen bonding. The peaks are characteristic of IR-active fundamental and combination lattice modes of crystalline Cr and Fe oxides[35]. The bands in 800-400 cm^{-1} region could be assigned to Fe-O or Cr-O lattice vibration[36-41]. The band at 947 cm^{-1} is assigned to Cr-O-Cr vibrations. The bands at 897 cm^{-1} is assigned to Cr-O-Cr vibrations and Fe-O-Fe[22,35]. The deviation from the unsupported

TABLE-1.
d-SPACINGS CORRESPONDING TO THE MOST SIGNIFICANT PEAKS IN THE XRD PATTERNS
OF THE SUPPORTED BINARY Fe-Cr OXIDES (THE 100 % INTENSITY IS IN BOLD)

Composition	d-Spacings								
α-Fe_2O_3	–	–	–	**2.67**	2.49	–	–	1.68	1.48
Cr_2O_3	–	–	–	2.63	2.45	–	–	**1.66**	1.42
Fe-Cr-Al-30	–	3.62	–	2.66	**2.48**	–	1.81	1.67	–
Fe-Cr-Si-30	4.20	3.59	**3.31**	2.65	2.47	–	1.87	1.67	–
Fe-Cr-Ti-30	–	–	**3.24**	2.66	2.48	2.18	–	1.69	–

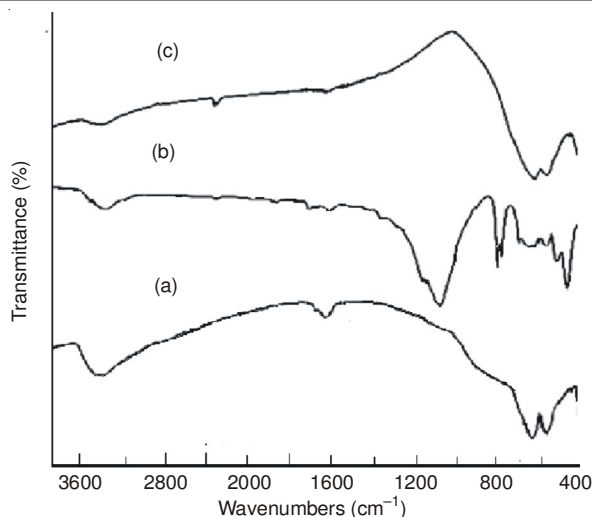Fig. 2. FTIR spectra of supported Fe-Cr binary oxides calcined at 750 ºC: (a) Fe-Cr-Al-30; (b) Fe-Cr-Si-30; (c) Fe-Cr-Ti-30

mixed oxides, α-Fe_2O_3/Cr_2O_3 may suggest that some iron and chromium ions are dispersed into the support matrix.

Change in the activity of catalyst with time on stream: The dehydrogenation of EB was performed in the presence of CO_2 as a mild oxidant over the supported Fe-Cr oxide catalysts. The overall EB conversion and the selectivity of the products for the different catalysts were studied. Fig. 3 showed that the time-on-stream experiments revealed that the EB conversion over Fe-Cr -Al decreased rapidly from 76.8 to 58.5 % after 7 h, whereas no evident decrease in the conversion is observed over Fe-Cr -Si and Fe-Cr -Ti catalysts after 4 h. The acidity of catalysts had significant impact on the catalytic performance. Strong acidity could promote the cracking of EB and make the styrene selectivity decrease. The deactivation of Fe-Cr-Al might not be due only to the coke formation, but also to the sintering of the catalyst. In fact, the evolution of the yield with time on stream for all these catalysts showed that they form the cracking products with almost the same yield (Fig. 4). The yield obtained over Fe-Cr-Al, Fe-Cr-Si and Fe-Cr-Ti are 3.7, 2.9 and 3.6 %, respectively. This result indicated that all the catalyst underwent the same effect of carbon deposition. Thus, the deactivation of Fe-Cr-Al might be due also to the sintering of the catalyst. This result was evidenced by SEM measurements. The morphological aspects of fresh and spent catalysts were evidenced by SEM images. As shown in Fig. 5a, fresh Fe-Cr -Al sample is characterized by irregular prismatic crystals. By contrast, spent Fe-Cr-Al catalyst is composed of large polygonal aggregates, particles (Fig. 5b). No significant carbon deposits are identified; only the solid structure was modified. Thus, CO_2 contributed in the carbon removal. In fact, Mamedov and Corberan[42] have reported that CO_2 has two main roles: first is to remove the hydrogen produced as water by the reverse water gas shift reaction; therefore, the equilibrium limitation of dehydrogenation shifts to the products side and the second is to remove the deposited coke.

The evolution of the styrene selectivity with time on stream is shown in Fig. 6. It can be seen that styrene is the major product in this reaction whereas benzene and toluene are minor by-products. After 7 h on stream, the Fe-Cr/Si and Fe-Cr/Ti
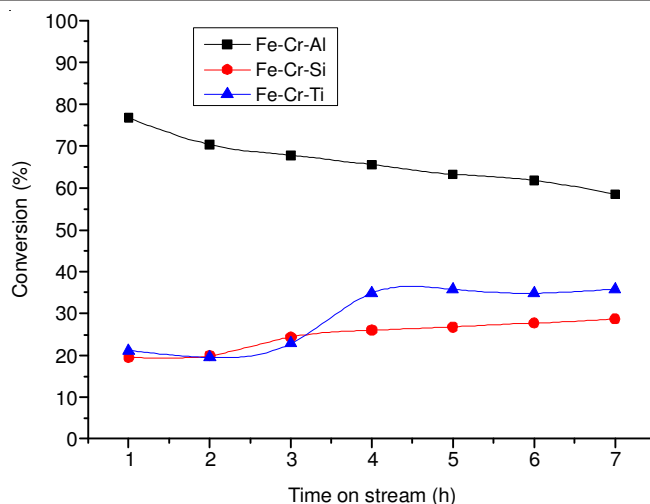

Fig. 3. Effect of the support on the EB conversion over supported Fe-Cr binary oxides catalysts as a function of reaction time. Reaction conditions: Temperature = 660 ºC, CO_2/EB = 11.7 (molar ratio) W/F = 13.9 g h/mol
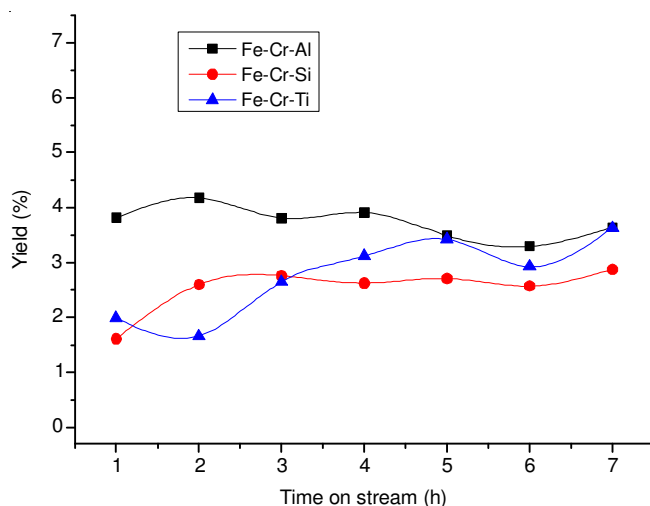

Fig. 4. Effect of the support on the styrene yield over supported Fe-Cr binary oxides catalysts as a function of reaction time. Reaction conditions: Temperature = 660 ºC, CO_2/EB = 11.7 (molar ratio) W/F = 13.9 g h/mol
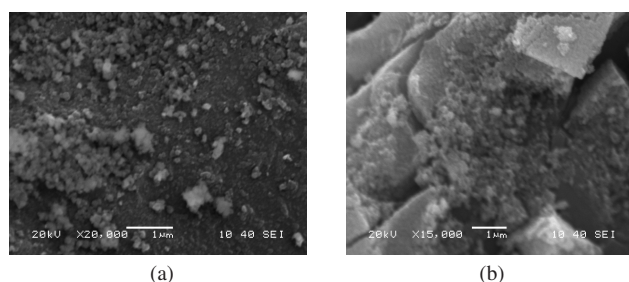

Fig. 5. SEM images of fresh and spent Fe-Cr-Al-30 catalysts. Reaction conditions: Temperature = 660 ºC, CO_2/EB = 11.7 (molar ratio) W/F = 13.9 g h/mol

catalysts exhibited almost identical styrene selectivity 90.0 and 90.9 %, respectively. The stability of styrene selectivity with time on stream while the activity decreased indicated that the catalyst deactivation was mostly due to sintering but not to carbon deposition (carbon deposition alters the styrene formation). Thus, besides its role as a soft oxidant, CO_2 played also the role of coke removal. As shown in Table-2, the Fe-Cr/Al
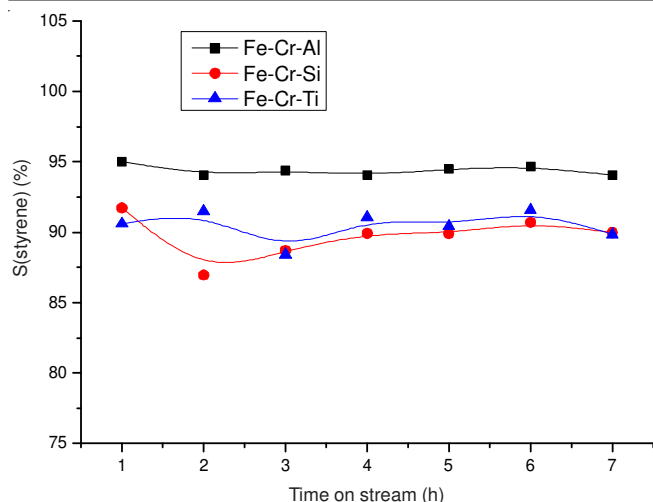
Fig. 6. Effect of the support on the styrene selectivity over supported Fe-Cr binary oxides catalysts as a function of reaction time

TABLE-2
CONVERSION AND SELECTIVITIES AT THE STEADY STATE
OBTAINED OVER SUPPORTED Cr-Fe BINARY OXIDES
CATALYSTS FOR THE EB DEHYDROGENATION WITH CO_2

Catalyst	Conversion (%)	Selectivity (%)		
		Styrene	Toluene	Benzene
Cr-Fe-Al	57.18	94.04	1.94	4.01
Cr-Fe-Si	29.70	91.98	2.15	5.87
Cr-Fe-Ti	33.55	89.35	3.48	7.17

Reaction conditions: Temperature = 660 ℃, CO_2/EB = 11.7 (molar ratio) and W/F = 13.9 g h/mol.

catalyst is the most active solid (conversion = 57.2 %) and the most selective in styrene (94.1 %). Its high activity compared to its counterpart silica and titania supported Fe-Cr oxides is due to the combined effects of acid-base and redox properties. The activity values suggest the following order of the favourable acid-base /redox and catalytic properties under these reaction conditions: Fe-Cr-Al > Fe-Cr-Ti > Fe-Cr-Si.

Effects of binary oxides loading on the catalytic activity of Fe-Cr-Al: It is well known that the conversion and selectivity to styrene is influenced by the acid-basic and redox properties of the catalyst. An optimum of configuration in acid-basic and redox properties needs to be tailored base on the binding energies in EB molecule. If the surface basic sites are strong enough to abstract b-hydrogen from EB, the break of the lateral C-C bond is promoted and, therefore, the selectivity to toluene will increase. If the catalyst surface acidity is larger, α-hydrogen can be abstracted from EB and the break of the phenyl-C bond become more probably, therefore, a higher selectivity to benzene will be obtained[33]. Since EB dehydrogenation occurs at the redox sites on the solid surface and CO_2 behaves as an oxidant for Fe and Cr species, it is useful to determine the optimal composition of the catalyst for dehydrogenation of EB with CO_2. For that purpose a series of Fe-Cr-Al catalysts with different Fe-Cr content (10, 30, 50, 70 and 90 wt %) marked as Fe-Cr-Al-x (x denotes the weight percent of Fe-Cr in Fe-Cr-Al) was prepared and tested. Fig. 7 represented the variation of the overall conversion of EB dehydrogenation as a function of time on stream over the series of catalysts. It can be seen that the EB conversion declined gradually with time on stream for low loadings while it remained stable for higher loadings
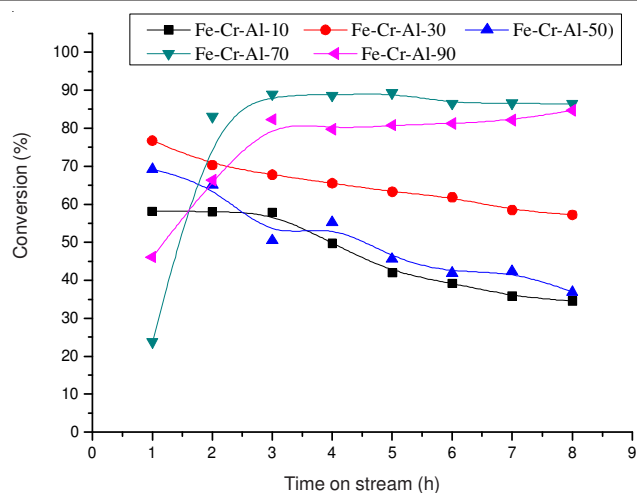

Fig. 7. Effect of Fe-Cr loading on the conversion of dehydrogenation of EB with CO_2 over alumina supported catalysts. Reaction conditions: Temperature = 660 ℃, CO_2/EB = 11.7 (molar ratio) and W/F = 13.9 g h/mol

(70 and 90 %). It is worth noting that the most stable catalysts were the less selective in styrene production (Fig. 8), *i.e.*, the most selective in cracking products. This result suggested that the main deactivation was not due to the coke formation as it was the case for many catalyst systems[22,43,44].
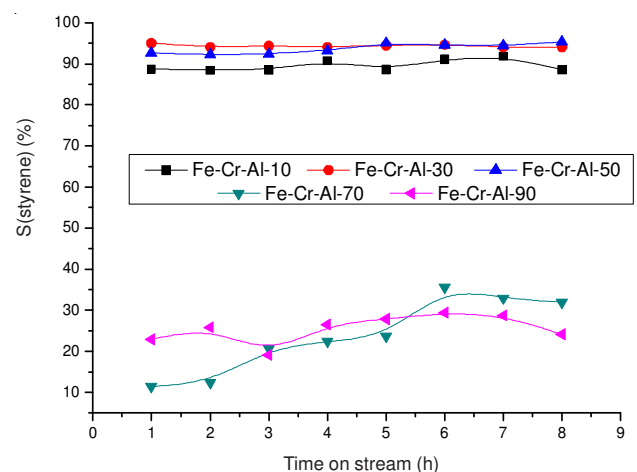

Fig. 8. Effect of Fe-Cr loading on the styrene selectivity for dehydrogenation of EB with CO_2 over alumina supported catalysts. Reaction conditions: temperature = 660 ℃, CO_2/EB = 11.7 (molar ratio) and W/F = 13.9 gh/mol

The activity and the selectivity at the steady state for dehydrogenation of EB in the presence of CO_2 are presented in the Fig. 9. It can be seen that the catalytic behavour of Fe-Cr/Al depends strongly on the loading. Ethylbenzene conversion initially increased from 31.93-95.38 % when Fe-Cr content increased from 10 to 70 %. Up to 70 % the EB conversion remained unchanged. As for the selectivities, Fig. 9 showed that the selectivity of styrene and the cracking products (benzene and toluene) remained unchanged when the loading varied from 10-50 %. A further increase in the binary oxides content decreased the styrene selectivity in favour of that of cracking. Thus, the optimal loading of the catalyst was determined to be 50 %.
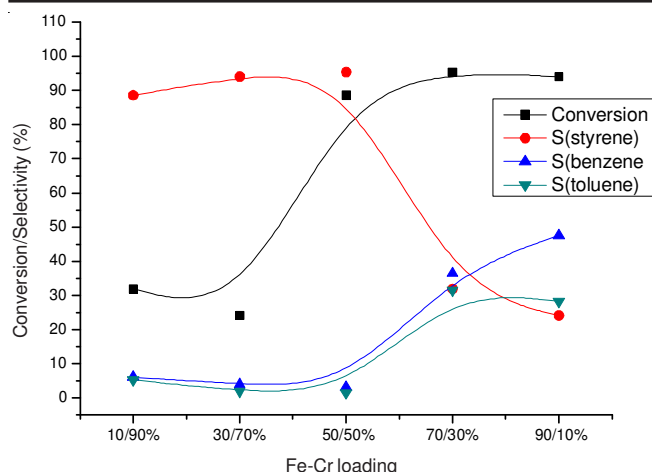
Fig. 9. Effect of Fe-Cr loading on the catalytic performance of Fe-Cr -Al catalysts for dehydrogenation of EB with CO_2. Reaction conditions: Temperature = 660 ℃, time = 7h, CO_2/EB = 11.7 (molar ratio) and W/F = 13.9 g h/mol

Conclusion

Compared to Fe-Cr-Si and Fe-Cr-Ti, Fe-Cr-Al is the suitable phase for the dehydrogenation of EB with CO_2. The activity value was observed in the following order : Fe-Cr-Al > Fe-Cr-Ti > Fe-Cr-Si. The variation of the Fe-Cr content in the Fe-Cr-Al catalyst systems indicated that the catalytic behaviour of Fe-Cr -Al catalyst was strongly dependent on the Fe-Cr content. The optimal loading of the catalyst was observed when Fe-Cr content was equal to 50 wt- %, which could be attributed to the appropriate acid- base sites distribution. Characterization of the spent Fe-Cr-Al catalyst indicated that that there are no significant carbonaceous deposits on the spent Fe-Cr-Al-30 catalyst, whereas modifications of its morphological aspect were observed. These results suggest that the main deactivation is not due to the coke formation as it is the case for many catalyst systems. Besides its role as a soft oxidant, CO_2 contributed in the carbon removal.

REFERENCES

1. E.H. Lee, *Catal. Rev.*, **8**, 285 (1973).
2. S.W. Chen, Z.F. Qin, A.L. Sun and J.G. Wang, *J. Nat. Gas Chem.*, **15**, 11 (2006).
3. A. Miyakoshi, A. Ueno and M. Ichikawa, *Appl. Catal. A*, **216**, 137 (2001).
4. A.A. Savoretti, D.O. Borio, V. Bucala and J.A. Porras, *Chem. Eng. Sci.*, **54**, 205 (1999).
5. F. Cavani and F. Trifiro, *Appl. Catal. A*, **133**, 219 (1995).
6. N. Mimura and M. Saito, *Catal. Today*, **55**, 173 (2000).
7. J. Matsui, T. Sodesawa and F. Nozaki, *Appl. Catal. A*, **67**, 179 (1991).
8. S.E. Park and S.C. Han, *J. Ind. Eng. Chem.*, **10**, 1257 (2004).
9. J.N. Park, J. Noh, J.S. Chang and S.E. Park, *Catal. Lett.*, **65**, 75 (2000).
10. C. Wang, W.B. Fan, Z.T. Liu, J. Lu, Z.W. Liu, Z.F. Qin and J.-G. Wang, *J. Mol. Catal. A: Chem.*, **329**, 64 (2010).
11. M. Ji, G. Chen, J. Wang, X. Wang and T. Zhang, *Catal. Today*, **158**, 464 (2010).
12. S.P.D. Marques, A.L. Pinheiro, T.P. Braga, A. Valentini, J.M. Filho and A.C. Oliveira, *J. Mol. Catal. A: Chem.*, **348**, 1 (2011).
13. M.S. Park, V.P. Vislovskiy, J.S. Chang, Y.G. Shul, J.S. Yoo and S.E. Park, *Catal. Today*, **87**, 205 (2003).
14. W. Bieniasz, M. Trebala, Z. Sojka and A. Kotarba, *Catal. Today*, **154**, 224 (2010).
15. A.H. de Morais Batista, F.F. de Sousa, S.B. Honorato, A.P. Ayala, J.M. Filho, F.W. de Sousa, A.N. Pinheiro, J.C.S. de Araujo, R.F. Nascimento and A. Valentini, *J. Mol. Catal. A: Chem.*, **315**, 86 (2010).
16. C.L. Lima, O.S. Campos, A.C. Oliveira, F.F. de Sousa, J.M. Filho, P.L. Neto, A.N. Correia, G.Q. Sabadia, I.M. Nogueira, G.S. Pinheiro and A.C. Oliveira, *Appl. Catal. A: Gen.*, **395**, 53 (2011).
17. C. Li, C. Miao, Y. Nie, Y. Yue, S. Gu, W. Yang, W. Hua and Z. Gao, *Chin. J. Catal.*, **31**, 993 (2010).
18. I.P. Belomestnykh, E.A. Skrigan, N.N. Rozhdestvenskaya and G.V. Isaguliants, *Stud. Surf. Sci. Catal.*, **72**, 453 (1992).
19. SS.S.E.H. Elnashaie, B.K. Abdallah, S.S. Elshishini, S. Alkhowaiter, M.B. Noureldeen and T. Alsoudani, *Catal. Today*, **64**, 151 (2001).
20. A. Aouissi, Z.A. Al-Othman and H. Bayahia, *Asian J. Chem.*, **22**, 4873 (2010).
21. S. Chen, Z. Qin, X. Xu and J. Wang, *Appl. Catal.* A, **302**, 185 (2006).
22. D. Hong, V.P. Vislovskiy, Y.K. Hwang, S.H. Jhung and J. Chang, *Catal. Today*, **131**, 140 (2008).
23. A. Sun, Z. Qin, S. Chen and J. Wang, *J. Mol. Catal. A: Chem.*, **210**, 189 (2004).
24. Y. Sakurai, T. Suzaki, K. Nakagawa, N. Ikenaga, H. Aota and T. Suzuki, *J. Catal.*, **209**, 16 (2002).
25. B.S. Liu, G. Rui, R.Z. Chang and C.T. Au, *Appl. Catal. A*, **335**, 88 (2008).
26. G. Carja, R. Nakamura, T. Aida and H. Niiyama, *J. Catal.*, **218**, 104 (2003).
27. X. Ye, N. Ma, W. Hua, Y. Yue, C. Miao, Z. Xi and Z. Gao, *J. Mol. Catal. A*, **217**, 103 (2004).
28. D.R. Burri, K.-M. Choi, D.-S. Han, Sujandi, N. Jiang, A. Burri and S.-E. Park, *Catal Today*, **131**, 173 (2008).
29. M. Saito, H. Kimura, N. Mimura, J. Wu and K. Murata, *Appl. Catal. A*, **239**, 71 (2003).
30. J.S. Chang, D.Y. Hong, Y.K. Park and S.E. Park, *Stud. Surf. Sci. Catal.*, **153**, 347 (2004).
31. Y. Sakurai, T. Suzaki, N. Ikenaga and T. Suzuki, *Appl. Catal. A*, **192**, 281 (2000).
32. N. Mimura, I. Takahara, M. Saito, T. Hattori, K. Ohkuma and M. Ando, *Catal. Today*, **45**, 61 (1998).
33. N. Dulamita, A. Maicaneanu, D.C. Sayle, M. Stanca, R. Craciun, M. Olea, C. Afloroaei and A. Fodor, *Appl. Catal. A*, **287**, 9 (2005).
34. A. Zecchina, S. Coluccia, E. Guglielminotti and G. Ghiotti, *J. Phys. Chem.*, **75**, 2774 (1971).
35. G. Arzamendi, V.A. de la Pena O'Shea, M.C. Alvarez-Galvan, J.L.G. Fierro, P.L. Arias and L.M. Gandia, *J. Catal.*, **261**, 50 (2009).
36. C.Y. Chen, C.K. Lin, M.H. Tsai, C.Y. Tsay, P.Y. Lee and G.S. Chen, *Ceramics Int.*, **34**, 1661 (2008).
37. L. Verdonck, S. Hoste, F.F. Roelandt and G.P. Van der Kelen, *J. Mol. Struc.*, **79**, 273 (1982).
38. P. Cambier, *Clay Miner.*, **21**, 191 (1986).
39. X. Xu, J. Wang, C. Yang, H. Wu and F. Yang, *J. Alloys Comp.*, **468**, 414 (2009).
40. Y. Hong, T.T. Pan, Y.P. Han, H.Z. Li, J. Ding and S.J. Han, *J. Magn. Magn. Mater.*, **310**, 37 (2007).
41. Z.M. Yao, Z.H. Li and Y. Zhang, *J. Colloid Interf. Sci.*, **266**, 382 (2003).
42. E.A. Mamedov and V.C. Corberán, *Appl. Catal. A*, **127**, 1 (1995).
43. K.N. Rao, B.M. Reddy, B. Abhishek, Y.H. Seo, N.Z. Jiang and S.E. Park, *Appl. Catal. B*, **91**, 649 (2009).
44. Y.Y. Qiao, C.X. Miao, Y.H. Yue, Z.K. Xie, W.M. Yang, W.M. Hua and Z. Gao, *Micropor. Mesopor. Mater.*, **119**, 150 (2009).